

Critical behavior at the ferromagnetic phase transition of $(\text{Fe}_{1-x}\text{Cr}_x)_{85}\text{B}_{15}$ metallic glasses close to the critical concentration of ferromagnetic long-range order

U. Güntzel and K. Westerholt

Institut für Experimentalphysik IV, Ruhr-Universität D-4630 Bochum, Federal Republic of Germany

(Received 7 June 1989)

The critical behavior of metallic glasses from the system $(\text{Fe}_{1-x}\text{Cr}_x)_{85}\text{B}_{15}$ is studied by measurements of the specific heat, the thermal derivative of the resistivity $d\rho/dT$, the ac susceptibility, and the magnetization in magnetic fields up to 1 T. The absence of a resolvable specific-heat anomaly and a smooth peak in $d\rho/dT$ indicates that the metallic glasses exhibit nonuniversal, smeared phase transitions. Nevertheless the magnetization data $M(H, T)$ at high fields show scaling of good quality with effective critical exponents similar to those found in other metallic-glass systems. The Curie temperature determined by the analysis of scaling, however, falls into the temperature range where the low-field magnetic hysteresis measurements clearly show the existence of hysteresis and spontaneous magnetization. The anomalous behavior at the phase transition is attributed to the existence of Fe-Cr concentration fluctuations on a length scale much larger than the random atomic short-range disorder.

INTRODUCTION

In this paper we study the magnetic phase transitions of samples from the metallic-glass system $(\text{Fe}_{1-x}\text{Cr}_x)_{85}\text{B}_{15}$ for concentrations down to the critical concentration for ferromagnetic long-range order $x_c \approx 0.3$. The weakly anisotropic ferromagnetic metallic glasses belong to the three-dimensional (3D) Heisenberg universality class with a specific-heat critical exponent $\alpha \approx -0.1$. General scaling arguments show that in this case random disorder does not change the asymptotic critical exponents (Harris criterion¹). High-temperature series expansion calculations,² renormalization-group calculations,^{3,4} and a more recent field-theoretical calculation⁵ corroborate this argument.

A different renormalization-group calculation,⁶ however, predicted that the critical behavior should definitely change in systems with random disorder. In the limit of strong disorder at the percolation limit the authors found a new fixed point with exponents identical to those of the spherical model with the numerical values $\alpha = -1$, $\beta = 0.5$, $\gamma = 2$, and $\delta = 5$ for the exponents of the specific heat, spontaneous magnetization, susceptibility, and isothermal magnetization at T_c , respectively. The crossover between this fixed point and the asymptotically stable 3D Heisenberg fixed point determines the critical behavior for the concentration range intermediate between the homogeneous compound and the percolation threshold. Recent crossover scaling calculations⁷ of the same group demonstrated that the crossover range can be described by effective exponents intermediate between those of the homogeneous fixed point and the random fixed point. Close to x_c the effective exponents can be well defined over a wide range in reduced temperatures. The crossover to the Heisenberg exponents is expected to occur at rather low reduced temperatures of typically $\tau \leq 10^{-3}$.

The critical behavior of ferromagnetic metallic glasses,

which are ideal systems for the experimental study of phase transitions in systems with random disorder, has been studied by many authors in the past decade.⁸⁻¹⁸ In the early investigations many authors derived effective exponents different from the 3D Heisenberg values with scaling of the magnetization over a large range in reduced temperatures.⁸⁻¹¹ More recently systematic investigations of ferromagnetic metallic glasses, including the reduced temperature range $\tau \leq 10^{-2}$, indicated that the crossover to the Heisenberg exponents occurs at reduced temperatures of about $\tau = 10^{-2}$.¹¹⁻¹⁶ At higher temperatures the effective exponent γ exhibits a broad maximum. To the opinion of some authors the effective exponents derived from the scaling plots over a large temperature range are the mean value of the temperature-dependent effective exponents, and the scaling of the magnetization data should improve when taking the Heisenberg exponents in temperature range $\tau \leq 10^{-2}$.^{18,19}

A serious problem one has to consider when studying phase transitions in systems with structural disorder is the question whether the topological or substitutional short-range disorder is the only relevant parameter describing the structure. Only in this case the experimental systems directly correspond to the theoretical models. If besides the random short-range disorder there are concentration or density fluctuations on a larger length scale the situation is more complex. Principally a thermodynamic phase transition can still exist, but the asymptotic critical behavior, which can only be observed if the correlation length is larger than the spatial correlations of the density fluctuations, can shift to unmeasurably low reduced temperatures. In recent years it became clear that metallic glasses are not as homogeneous as has often been assumed. Low-angle x-ray scattering experiments,²⁰ field-ion-emission spectroscopy,²¹ and neutron scattering studies²² revealed that many metallic glasses possess density or concentration fluctuations with a spatial correla-

tion between several ten and several hundred Å. Microscopic methods like Mössbauer spectroscopy²³ gave strong indications of a nonrandom distribution of metal atoms. Unfortunately the conclusions about the critical behavior of ferromagnetic metallic glasses rely mainly on the analysis of the magnetization data $M(H, T)$ either by an analysis of modified Arrott plots or by an analysis of the scaling. As will be shown, the inherent ambiguities of these methods make them rather insensitive for detecting the influence of metallurgical inhomogeneities.

The magnetic specific heat at the ferromagnetic phase transition, on the other hand, is a very sensitive probe for metallurgical inhomogeneities. The critical behavior of the specific heat has rarely been analyzed in metallic glasses, since the specific-heat peak at the magnetic transition is rather small and difficult to analyze with the necessary precision. There is one systematic study of the specific-heat peak at the magnetic phase transition of metallic glasses,²⁴ however, which bears some important consequences. The authors find that in $\text{Fe}_{80}\text{P}_{13}\text{C}_7$ a sharp specific-heat peak exists. The substitution of up to 10 at. % Ni for Fe leaves the form of the peak essentially unchanged. With the substitution of 2 at. % Cr or Mn for Fe, however, the peak is strongly smeared and a well-defined critical behavior no longer exists. The authors fitted this smooth peak by assuming a Gaussian distribution of T_c values. This smearing is probably due to non-random concentration fluctuations of the Cr or Mn atoms.

In this paper we study in detail the specific heat, thermal derivative of the resistivity, low-field magnetic hysteresis properties, ac susceptibility, and magnetization isotherms of Fe-Cr-B metallic glasses. We will show that the influence of the inhomogeneity of the system, which is rather obvious in the specific heat, is not at all obvious in the magnetic quantities. Only a detailed analysis reveals the anomalous behavior at the phase transition and points towards the nonuniversal character of the phase transition. This has some implications for the critical behavior of other metallic glass systems reported in the literature, many of which probably belong to the class of slightly inhomogeneous systems, where the influence of the inhomogeneity is not as strong as in the Fe-Cr-B metallic glasses but nevertheless is important for the critical behavior.

PREPARATION AND EXPERIMENTAL

The metallic glasses of this study were prepared by standard melt spin technique in pure Ar atmosphere. The amorphous structure was checked by x-ray analysis. For the magnetic measurements a ribbon of about 20 cm total length was selected. A possible concentration gradient along the ribbon could be excluded by comparing the ac susceptibility of two pieces cut from both ends of the sample. For the ribbons selected for the experiments the ac susceptibility was identical within the experimental precision and thus a macroscopic concentration gradient could be neglected. About 10 cm of the ribbon was wound into toroidal shape and used for the low-field magnetic hysteresis measurements. The rest of the ribbon

was used for the other experiments. The measurements we report on below were normally done in the as-quenched and the annealed state of the sample. The annealing of the samples was done at 680 K for 3 h. The as-quenched and the annealed sample state is denoted by series 1 (*s1*) and series 2 (*s2*) samples in the figures.

For the measurements of the magnetic hysteresis loops a primary and a secondary coil of Cu wire was wound onto the toroids and used for field generation and signal pickup. The hysteresis loops were measured quasistatically at a frequency of about 10^{-1} s^{-1} using a sensitive electronic integrator (Walker fluxmeter type MF-3A). The ac susceptibility was measured on the same toroids by mutual inductance technique with an amplitude of the generating field of 10^{-3} A/cm at a frequency of 33 s^{-1} . The voltage induced in the secondary windings was measured by lock-in technique; the typical resolution we could achieve was 10^{-5} of the signal at the Hopkinson maximum.

The specific heat of the samples was measured by an ac technique with optical heating of the sample. The basis for this technique²⁵ is the fact that the temperature oscillation generated when heating the sample with chopped light of the frequency ω is proportional to the reciprocal specific heat, if the frequency is small compared to the reciprocal inner relaxation time and large compared to the reciprocal outer relaxation time, and the thermal conductivity between the sample and the thermometer is large compared to the thermal conductivity between sample and bath. In our experiment the temperature was measured by a thermocouple spot welded to the sample surface and the sample was coupled weakly to the sample holder by thermally conducting grease. The preceding conditions were fulfilled to a good approximation at a frequency $\omega = 7 \text{ s}^{-1}$. The ac technique has the advantage of a continuous output signal and a high resolution even with a small sample mass. In our experiment the total mass of the sample was about 1 mg and we achieved a resolution of about 10^{-3} close to the maximum of the specific heat.

With some modifications the same experimental set up was used for a direct measurement of the thermal derivative of the resistivity $d\rho/dT$. Four Cu wires are attached to the sample by silver epoxy and a constant dc current flows through the outer current contacts. The sample is heated by chopped light and the ac signal generated at the inner voltage contacts is directly proportional to the ac amplitude of the temperature and to $d\rho/dT$. The ac signal is decoupled capacitively and measured by lock-in technique. This direct electronic differentiation allows a very high resolution of the fine structure in $d\rho/dT$, which would correspond to a resolution of about 10^{-7} in a direct measurement of ρ followed by a numerical differentiation in order to determine $d\rho/dT$.

The magnetization of the samples in high magnetic fields was measured by a vibrating sample magnetometer (PAR 160). Five pieces of the ribbon of 1 cm length were placed in parallel on the sample holder and thermally coupled to the GsAs thermometer by a bundle of thin Cu wires. In this sample geometry the maximum demagnetizing field is below 10 Oe. The effective demagnetizing

factor was determined from the slope of the $M(H)$ curve at low fields at a temperature of 4.2 K.

Since for the discussion in the following the comparison of the magnetic ordering temperatures determined by the different experiments is essential, the thermometers were calibrated against one standard Pt thermometer. The relative accuracy of the temperature measurements in the different experiments thus is better than 0.2 K.

RESULTS AND DISCUSSION

In Fig. 1 we show the magnetic phase diagram we have determined for the metallic glass system $(\text{Fe}_{1-x}\text{Cr}_x)_{85}\text{B}_{15}$. In the as-quenched state the reentrance phase line and the paramagnetic phase line intersect at a critical concentration $x_c=0.33$, in the annealed state the ordering temperatures shift to lower values by about 30 K and the critical concentration is at $x_c=0.31$. The analysis of the hyperfine field distribution in Fe-Cr metallic glasses²³ showed that the Fe atoms lose their magnetic moment when they have more than four Cr nearest neighbors. Cr is assumed to be nonmagnetic in the concentration range of the phase diagram in Fig. 1. Thus x_c can be interpreted as a percolation threshold for Fe atoms having a magnetic moment.

The results of the measurements of the temperature dependence of the magnetic hysteresis loops in the annealed state of the samples are summarized in Figs. 2(a) and 2(b). Both the remanent magnetization and the coercive force vanish critically for $T \rightarrow T_c$. Empirically one can fit power laws like $M_r(T) \propto (T_c - T)^y$ but y is known to be no pure critical exponent (see Ref. 26 for measurements on Ni) and does not coincide with the critical exponent of the spontaneous magnetization β . We only use the extrapolation shown in Fig. 2 for a first determination of the ferromagnetic Curie temperature (Table I).

In Fig. 3 we show the results of the ac susceptibility on the same samples. One observes a sharp Hopkinson max-

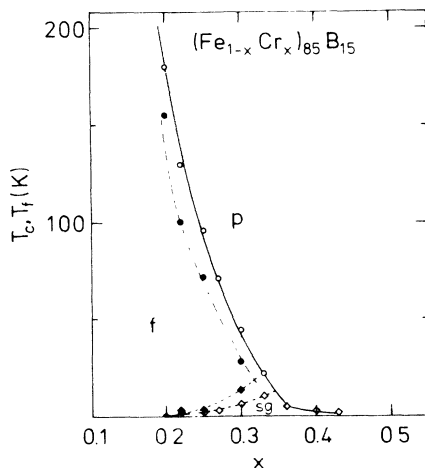


FIG. 1. Magnetic ordering temperature as a function of the Cr concentration for samples $(\text{Fe}_{1-x}\text{Cr}_x)_{85}\text{B}_{15}$; f: ferromagnetic; p: paramagnetic; sg: spin glass; full line: as-quenched state of the sample (s1); dashed line: annealed state of the sample (s2).

imum with the ferromagnetic Curie temperatures as determined from the onset of the spontaneous magnetization at the high-temperature side of the peak. For a well-defined ferromagnetic phase transition the analysis of the ac susceptibility principally allows the determination of the critical susceptibility exponent γ . From the standard power law for the susceptibility one gets by differentiation

$$-(d \ln \chi / dT)^{-1} = \gamma^{-1} (T - T_c). \quad (1)$$

Thus by numerical differentiation of the susceptibility one can determine the critical exponent γ and the Curie temperature T_c . The result of this analysis for some of our measurements is shown in Fig. 4. One finds a straight line behavior at higher reduced temperatures as expected from Eq. (1) with a strong deviation at about 1–4 K above the extrapolated T_c . The effective ex-

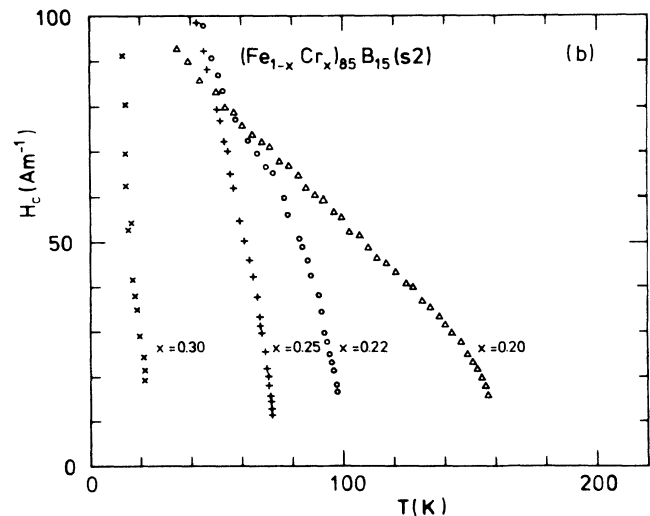
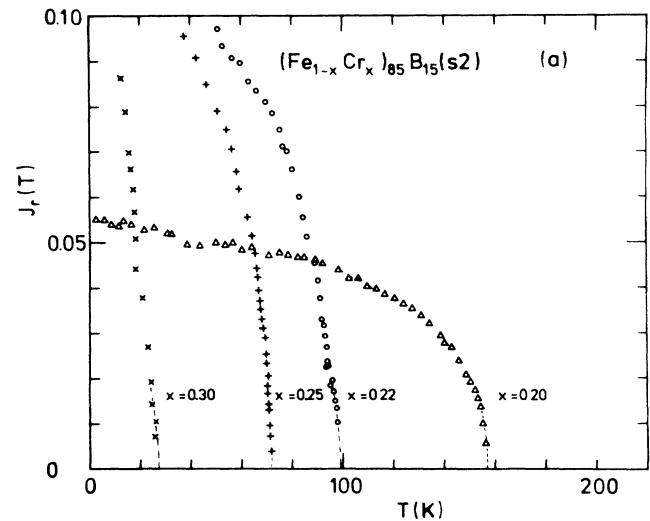


FIG. 2. Remanent polarization (a) and coercive force (b) for samples $(\text{Fe}_{1-x}\text{Cr}_x)_{85}\text{B}_{15}$ as a function of temperature. The extrapolation towards $J_r=0$ (dashed line) gives the ferromagnetic Curie temperature of the second row Table I.

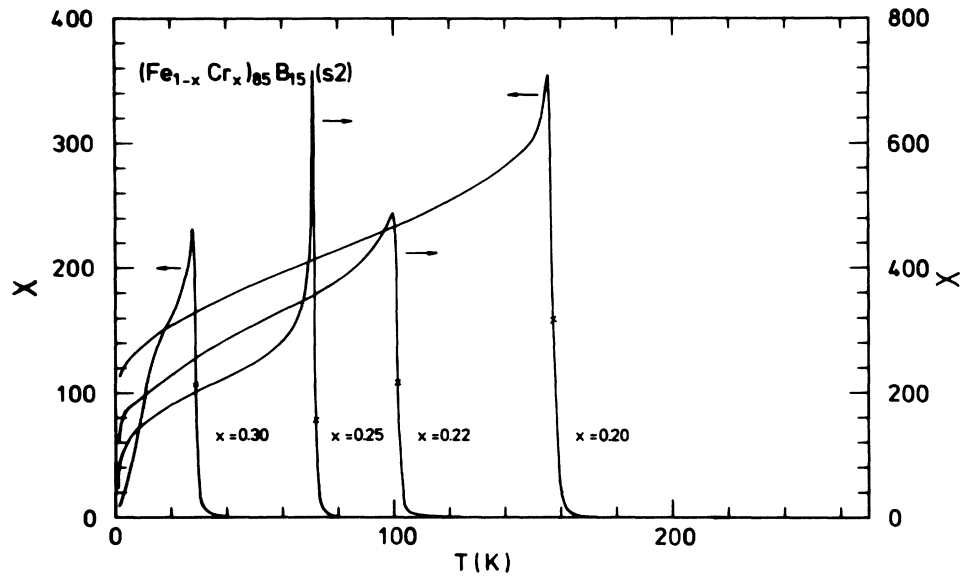


FIG. 3. Ac susceptibility for samples $(\text{Fe}_{1-x}\text{Cr}_x)_{85}\text{B}_{15}$ as a function of temperature. The crosses mark the ferromagnetic Curie temperatures from Fig. 2.

ponents turn out to be strongly preparation dependent and do not vary systematically with the concentration. Moreover the extrapolated value for T_c is inconsistent with T_c determined from the onset of spontaneous magnetization (indicated by the vertical arrow in Fig. 4). Thus we conclude that the temperature dependence of the ac susceptibility does not follow a pure critical power law and the effective exponents given in the figure have essentially no meaning. Since even in metallic glasses with better defined phase transitions¹²⁻¹⁷ the magnetization data at low fields deviate from scaling and universal behavior, the ac susceptibility measured at very low fields is not well suited for an analysis of critical behavior in metallic glasses.

In Fig. 5 we show the results of our analysis of the specific heat close to the ordering temperature. For none of the samples a peak in the specific heat can be resolved. This is consistent with the results of the specific-heat measurements of Ref. 24 for Fe-Cr metallic glasses with lower Cr content. These authors observed a strongly in-

creasing smearing of the specific-heat peak with increasing Cr concentration. For their maximum Cr concentration of about 10 at. % only a very small peak with an estimated width of 10 K for the distribution of T_c values was left. Extrapolating their results towards our Cr concentrations above 20 at. % the absence of a resolvable specific-heat peak in our measurements is not unexpected.

In this situation the measurement of the thermal derivative of the resistivity, which can be done with a much higher resolution than the specific heat, can be helpful. From the theoretical work^{27,28} it is expected that the scattering of conduction electrons by the critical fluctuations at the phase transition leads to a peak in the thermal derivative of the resistivity. Close to the ordering temperature $d\rho/dT$ is expected to be proportional to the magnetic specific heat. Thus close to T_c one expects

$$d\rho/dT = A(T - T_c)^{-\alpha} + B \quad (2)$$

TABLE I. Ferromagnetic ordering temperatures determined from the low-field hysteresis measurements (second row) and the scaling analysis (third row) and the effective exponents determined from the scaling analysis. The first row gives the Cr concentration in the formula $(\text{Fe}_{1-x}\text{Cr}_x)_{85}\text{B}_{15}$.

Cr concentration	T_c (hysteresis)	T_c (scaling)	δ_{eff}	β_{eff}	γ_{eff}
0.20 as quenched	187.3±0.7	180.6±0.4	4.8±0.2	0.42±0.02	1.60±0.1
0.20 annealed	157.5±0.7				
0.22 as quenched	132.8±0.4				
0.22 annealed	98.4±0.6	98.5±0.3	4.9±0.2	0.44±0.02	1.70±0.1
0.25 as quenched	97.0±0.7				
0.25 annealed	72.2±0.4	68.0±0.2	5.1±0.15	0.44±0.03	1.80±0.15
0.30 as quenched		42.2±0.2	5.2±0.1	0.46±0.03	1.90±0.20
0.30 annealed	27.0±0.3				

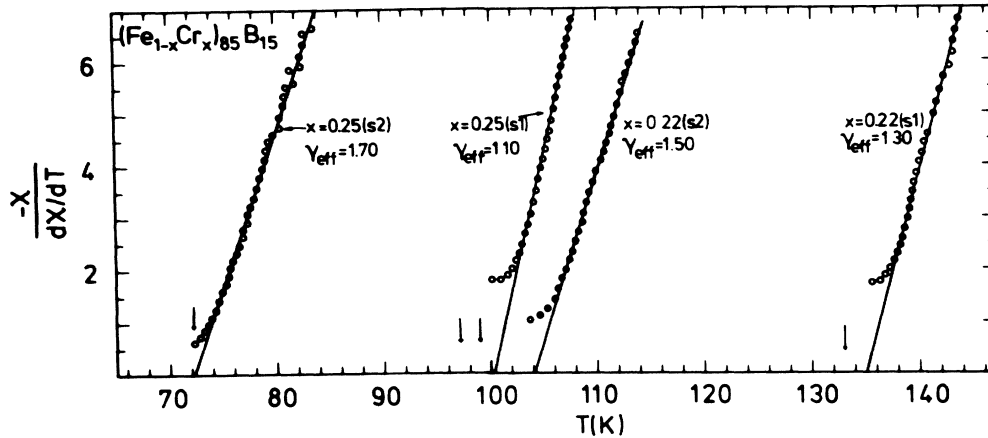


FIG. 4. Kouvel-Fisher plots for samples $(\text{Fe}_{1-x}\text{Cr}_x)_{85}\text{B}_{15}$. The slope of the straight line gives the effective susceptibility exponent γ_{eff} , the vertical arrows mark the Curie temperatures from Fig. 2.

and

$$d\rho/dT = A'(T_c - T)^{-\alpha} + B' \quad (2')$$

for $T \geq T_c$ and $T \leq T_c$, respectively.

For many metallic ferromagnets including Fe and Ni and different metallic glasses, a cusp of the form given by Eq. (2) has been observed. It turned out, however, that reliable values for the critical exponent α are difficult to obtain from a fit of the $d\rho/dT$ curves.²⁹

The results of the thermal derivative of the resistivity measured by direct electronic differentiation are given in Fig. 6(b). For comparison and in order to demonstrate the high experimental resolution we show the measurement of a Fe-Ni metallic glass in Fig. 6(a). In the Fe-Ni metallic glass one observes a sharp peak at the ordering temperature indicating the existence of a well-defined

phase transition. But unlike the specific-heat peak in metallic glasses, which is approximately symmetric for $T \geq T_c$ and $T \leq T_c$, the peak in $d\rho/dT$ is unsymmetric, being very flat for $T \leq T_c$. This indicates that the temperature range where the proportionality of c and $d\rho/dT$ holds is very narrow in metallic glasses and confined to a temperature range $\tau \leq 10^{-2}$.

For Fe-Cr-B metallic glasses in Fig. 6(b) one observes a broad, smooth peak in $d\rho/dT$ with the ferromagnetic Curie temperature determined from the low-field hysteresis measurements at the low-temperature side of the peak (indicated by vertical arrows in the figure). The peak compares well with the specific-heat measurements of Ref. 24 for Fe-Cr metallic glasses with lower Cr content. We thus conclude that the broad peak in $d\rho/dT$ is due to the critical scattering at a strongly smeared phase transition. Interestingly the sharp kink in $d\rho/dT$, which is observed at the low-temperature side of the peak, coincides with the Hopkinson maximum in the ac susceptibility and thus seems to be caused by the magnetic anisotropy.

We next turn the results of the analysis of the magnetization measurements in the field range from 5 mT to 1 T. The critical behavior is analyzed as follows: The isotherms are first plotted on a double logarithmic scale in order to find the critical isotherm $m(H) = BH^{1/\delta}$ for $T = T_c$. The example in Fig. 7 for the sample with $x = 0.20$ in the as-quenched state thus gives $T_c = 180.6$ K and $\delta = 4.8$. Next we apply the empirical equation of state proposed by Arrott and Noakes.³⁰ We plot the magnetization isotherms following the equation:

$$(M/M_0)^{1/\gamma} = A(H)^{1/\beta} + c(T - T_c). \quad (3)$$

The critical exponent β and γ are chosen in order to get a linear representation of the isotherms, as a constraint the critical isotherm must intersect the axes at the origin. As shown in Fig. 8, the magnetization isotherms with the effective exponents properly chosen are well represented by straight lines for higher magnetic fields but show a curvature for lower fields. The magnetic field where the

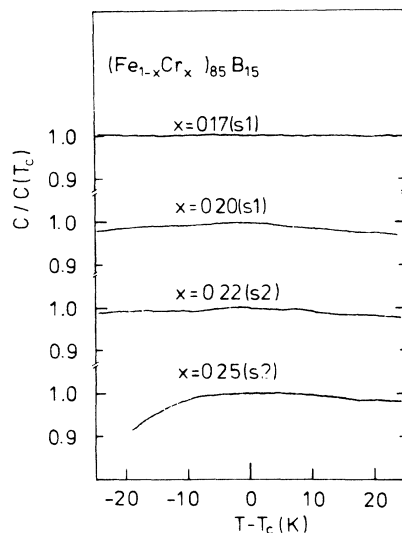


FIG. 5. Relative specific heat as a function of temperature for samples $(\text{Fe}_{1-x}\text{Cr}_x)_{85}\text{B}_{15}$. $c(T_c)$ denotes the specific heat at the ordering temperature.

first deviation is observed is 150 Oe typically. The critical exponents for the spontaneous magnetization β_{eff} and the susceptibility γ_{eff} are then determined by extrapolating the isotherms linearly and plotting the spontaneous magnetization and the zero-field susceptibility on a double logarithmic scale.

An important test for the validity of the exponents is the scaling of the magnetization data. From general

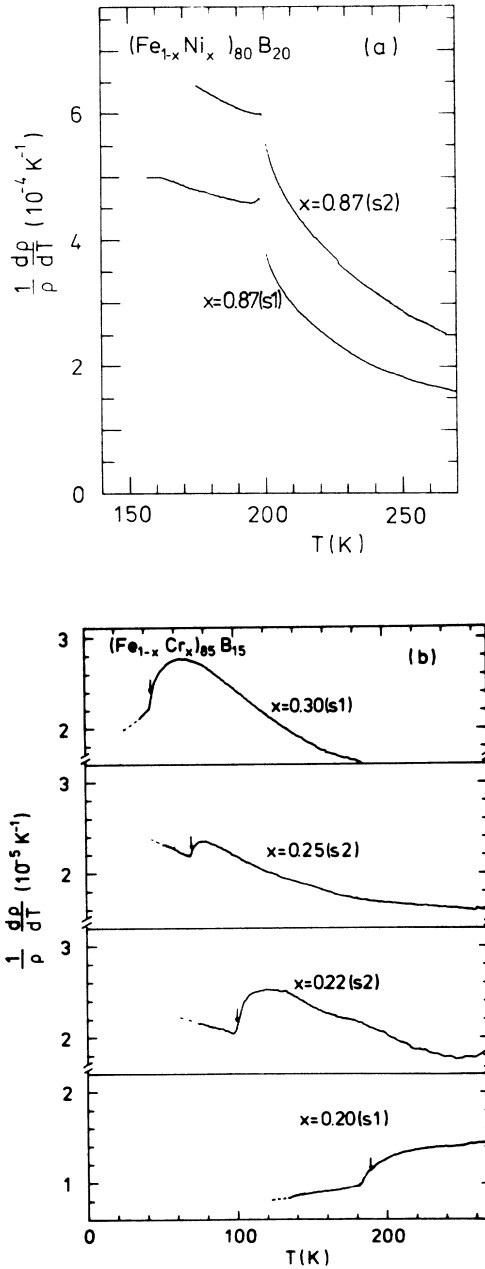


FIG. 6. Thermal derivative of the electrical resistivity vs temperature for a sample from the $(\text{Fe}_{1-x}\text{Ni}_x)_{80}\text{B}_{20}$ -system [Fig. 6(a)] and for samples $(\text{Fe}_{1-x}\text{Cr}_x)_{85}\text{B}_{15}$ [Fig. 6(b)]. The arrows in Fig. 6(b) mark the magnetic ordering temperature from Fig. 2.

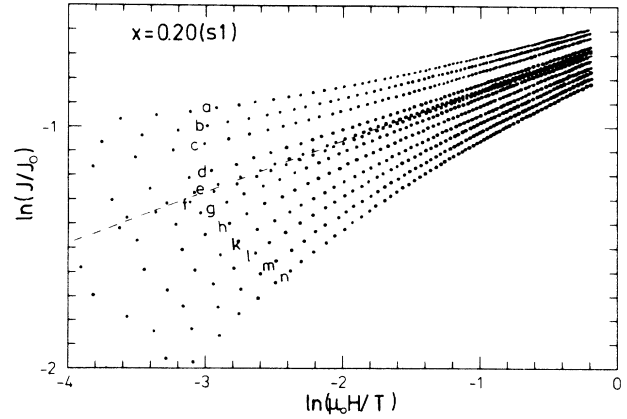


FIG. 7. Isothermal magnetic polarization vs magnetic field on a double logarithmic scale for the sample $(\text{Fe}_{0.80}\text{Cr}_{0.20})_{85}\text{B}_{15}$. The dashed line marks the critical isotherm. The letters denote the temperature of the sample: (a):169.8 K, b:172.8 K, c:175.0 K, d:178.8 K, e:180.3 K, f:181.0, g:182.2 K, h:183.9 K, k:185.7 K, l:187.3 K, m:189.0 K, n:190.6 K, o:192.2 K, p:193.7 K).

scaling arguments the magnetization data should collapse on two branches when plotted in the scaled form

$$M/\tau^\beta = f_{+,-}(H/\tau^{\beta\delta}) \quad (4)$$

with the plus sign for $T \geq T_c$ and the minus sign for $T \leq T_c$. We have tested the scaling of the magnetization data beginning with the set of exponents and the Curie temperature by the modified Arrott plots. Scaling only holds for values in a narrow range close to the values determined by the modified Arrott plots (Fig. 9). The range of validity of the parameters thus determined is given by the error bars in Table I.

The same analysis was done for the samples with different concentrations. A scaling of similar quality as in Fig. 9 is found for all samples independent of the sam-

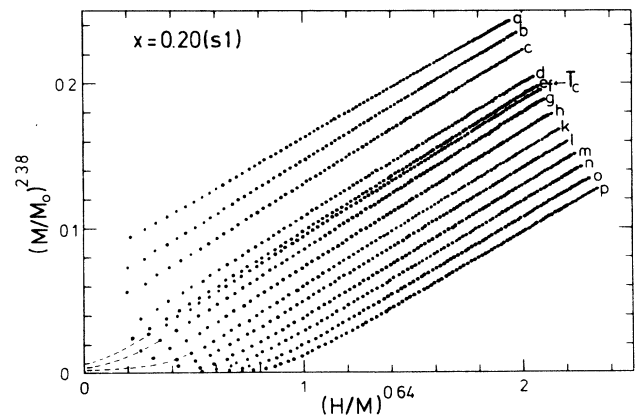


FIG. 8. Modified Arrott plots for magnetization isotherms close to T_c for the sample $(\text{Fe}_{0.80}\text{Cr}_{0.20})_{85}\text{B}_{15}$. The dashed line indicates schematically the continuation of the isotherms for very low magnetic fields (see the main text). The temperatures for the isotherms are the same as given in Fig. 7.

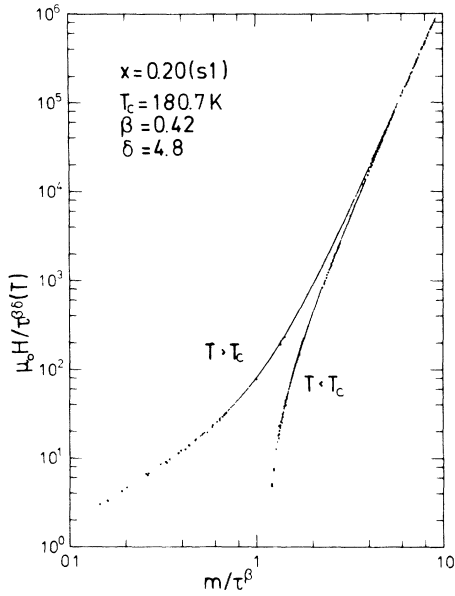


FIG. 9. Magnetization isotherms from Fig. 8 in scaled form. The values for the parameters T_c , β , and δ of the plot are given in the figure.

ple state whether annealed or as quenched, Figs. 10 and 11 show some examples. The only exception is the sample with $x = 0.30$ with a Curie temperature of 27 K and a concentration very close to x_c . For this sample a scaling representation of the magnetization could not be found. The effective critical exponents thus determined are given in Table I, the numerical values for these exponents are similar to those derived from the scaling analysis in a wide temperature range for other metallic glasses.¹⁰⁻¹⁸ The effective exponents are concentration dependent and the deviation from the Heisenberg exponents increases for $x \rightarrow x_c$. Contrary to the example given in Ref. 18 the scaling cannot be improved with the Heisenberg exponents for the range of reduced temperature $\tau \leq 10^{-2}$.

When comparing the Curie temperature from the low-field and the high-field measurements in Table I, one finds a severe contradiction. In every case the Curie temperature derived from the Arrott plots and the scaling analysis of the high-field data is lower than the value determined from the low-field magnetization measurements. One observes that the difference of the two Curie temperatures is larger for the samples in the as quenched and thus more inhomogeneous state and reaches values up to 6 K here.

The comparison of the high-field and the low-field data of the magnetization reveals that the continuation of the magnetization isotherms towards very low fields will follow the dashed lines drawn in Fig. 8 schematically. Even for temperatures of several K above the extrapolated T_c the isotherms intersect the magnetization axis at finite values for the spontaneous magnetization. The magnetization values from this strongly curved part of the magnetization isotherms would strongly deviate from the universal plot in Fig. 9.

Now, it is well known that the experimental magneti-

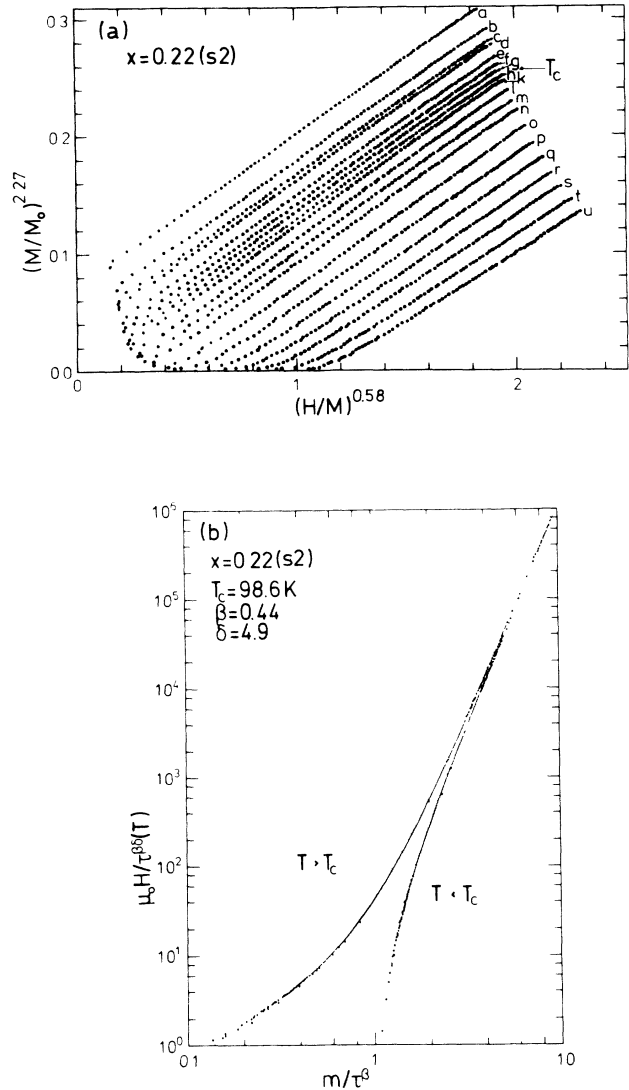


FIG. 10. Modified Arrott plots (a) and scaled plots of the magnetization (b) for the sample $(\text{Fe}_{0.78}\text{Cr}_{0.22})_{85}\text{B}_{15}$ (a:91.2 K, b:93.5 K, c:94.7 K, d:95.2 K, e:96.5 K, f:97.4 K, g:98.0 K, h:98.7 K, k:99.2 K, l:100.4 K, m:101.7 K, n:102.8 K, o:105.0 K, p:107.0 K, q:109.0 K, r:111.0 K, s:112.9 K, t:114.5 K, u:116.7 K).

zation values at low fields must be excluded from the scaling analysis for metallic glasses and other mixed compounds. For temperatures $T < T_c$ the existence of magnetic domains is the obvious reason for this, for temperatures $T > T_c$ the situation is more difficult. Two problems can make the magnetization values unreliable at low fields even for temperatures in the paramagnetic range: First, the correction of the demagnetizing field, which becomes very important for low applied fields, can only be done approximately. Second, the low-field data are very sensitive towards any type of heterogeneity as, e.g., ferromagnetic impurity phases. These two factors are eliminated by extrapolating the isotherms in the modified Arrott plots linearly. However, one expects that the extrapolation should give the correct value for T_c which is

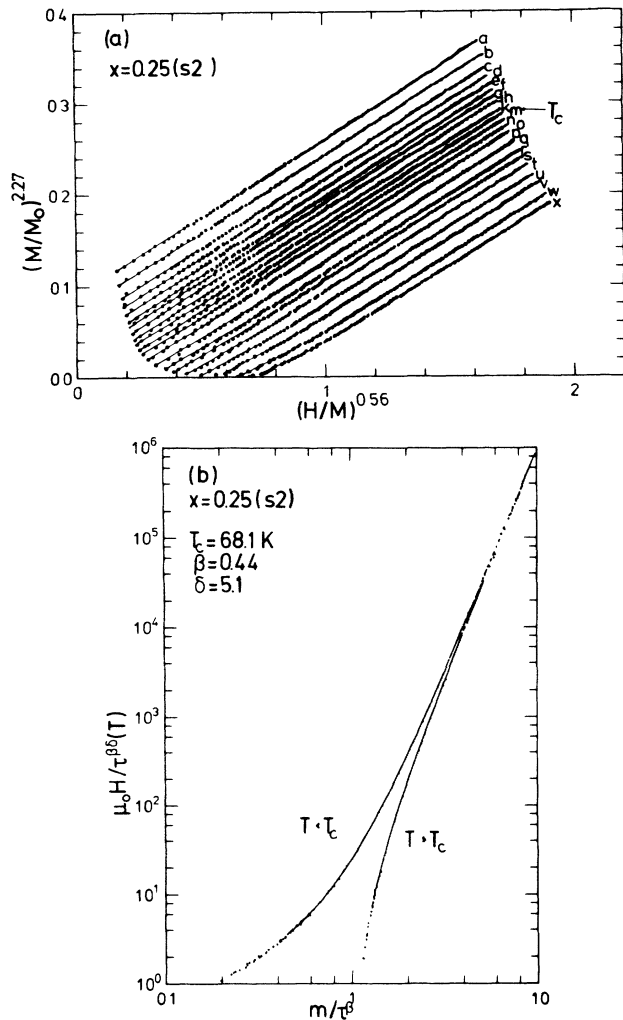


FIG. 11. Modified Arrott plots (a) and scaled plots of the magnetization (b) for the sample $(\text{Fe}_{0.75}\text{Cr}_{0.22})_{85}\text{B}_{15}$ (a:61.6 K, b:62.7 K, c:64.0 K, d:64.8 K, e:65.6 K, f:66.2 K, g:66.7 K, h:67.3 K, k:68.0 K, m:68.5 K, n:69.0 K, o:69.6 K, p:70.3 K, q:71.3 K, r:72.3 K, s:73.0 K, t:74.0 K, u:75.1 K, v:76.2 K, w:77.6 K, x:78.6 K).

consistent with T_c from low-field measurements. Our results and the discrepancy in T_c indicates a third and more serious possibility for the strong curvature of the Arrott plots at low fields, namely the absence of a well-defined phase transition.

SUMMARY AND CONCLUSIONS

The absence of a peak in the specific heat and the broad anomaly in the thermal derivative of the electrical resistivity clearly indicate that the Fe-Cr-B metallic glasses under study here exhibit a smeared ferromagnetic phase transition with nonuniversal character. The reason for this behavior, we suppose, are Fe-Cr concentration fluctuations on a length scale above 100 Å. Contrary to random short-range structural disorder, these concentration fluctuations are relevant for the phase transition in the whole experimentally accessible range of reduced temperatures.

The smooth peak in $d\rho/dT$ is contrasted by the results of the magnetic measurements, where the existence of a very sharp Hopkinson maximum and the sharp onset of the spontaneous magnetization in the low-field magnetic hysteresis measurements suggest the existence of a well-defined phase transition.

Similarly the good scaling behavior of the magnetization for magnetic fields above 100 Oe points towards the existence of a well-defined phase transition. Actually the scaling of the $M(H, T)$ data is as good as in any other metallic glasses published in the literature. For a smeared phase transition a scaling of the magnetization is rather unexpected but we mention that we have found similar behavior in the magnetically heterogeneous system $\text{Eu}_x\text{La}_{1-x}\text{S}$.³¹

It could be assumed that this scaling is purely accidental, i.e., that the three parameters of the scaling plot are sufficient for a reasonable data collapsing. However, the quality of the scaling and the numerical values of the effective exponents which fit well to those determined for other diluted Heisenberg magnets with better defined phase transitions³¹⁻³⁷ suggest that the scaling indicates the universal character of the phase transition in high magnetic fields. Thus the metallurgical inhomogeneity seems to be an irrelevant parameter in the renormalization-group theoretical sense for high magnetic fields. The concentration dependence of the effective exponents for $x \rightarrow x_c$ in Table I ($\delta \rightarrow 5$ and $\beta \rightarrow 0.5$ for $x \rightarrow x_c$) is in qualitative agreement with the crossover scaling theory of Ref. 7 and the concentration dependence observed experimentally in the diluted Eu chalcogenides.³¹⁻³⁷

ACKNOWLEDGMENTS

The authors thank the Deutsche Forschungsgemeinschaft for financial support of this work within the Sonderforschungsbereich No. 166.

¹A. B. Harris, J. Phys. C 7, 1671 (1974).

²E. Brown, J. W. Essam, and C. M. Place, J. Phys. C 8, 321 (1975).

³G. Grinstein and A. Luther, Phys. Rev. B 13, 1329 (1976).

⁴A. Weinrib and B. I. Halperin, Phys. Rev. B 27, 413 (1983).

⁵J. Jug, Phys. Rev. B 27, 609 (1983).

⁶G. Sobotta and D. Wager, J. Phys. C 11, 1467 (1978).

⁷H.-O. Heuer and D. Wagner, J. Phys. (Paris) Colloq. 49, C8-

1265 (1988); Phys. Rev. B 40, 2502 (1989).

⁸K. Yamada, Y. Ishikawa, Y. Endoh, and T. Matsumoto, Solid-State Commun. 16, 1335 (1975).

⁹P-Gaunt, S. C. Ho, G. Williams, and R. W. Cochrane, Phys. Rev. B 23, 251 (1981).

¹⁰Z. Marohnic, D. Dobrac, E. Babic, and K. Zadro, J. Magn. Magn. Mater. 38, 93 (1983).

¹¹Y. Yeshurun, M. B. Salamon, K. V. Rao, and H. S. Chen,

- Phys. Rev. B **24**, 1536 (1981).
- ¹²S. N. Kaul, J. Magn. Magn. Mater. **53**, 5 (1985).
- ¹³W. U. Kellner, T. Albrecht, M. Fähnle, and H. Kronmüller, J. Magn. Magn. Mater. **62**, 169 (1986).
- ¹⁴M. Fähnle, J. Magn. Magn. Mater. **45**, 279 (1984).
- ¹⁵H. Haug, M. Fähnle, H. Kronmüller, and F. Haberey, Phys. Status Solidi B **144**, 411 (1987).
- ¹⁶W. U. Kellner, M. Fähnle, H. Kronmüller, and S. N. Kaul, Phys. Status Solidi B **144**, 397 (1987).
- ¹⁷M. Fähnle, J. Magn. Magn. Mater. **65**, 1 (1987).
- ¹⁸M. Fähnle, W. U. Kellner, and H. Kronmüller, Phys. Rev. B **35**, 3640 (1987).
- ¹⁹S. N. Kaul, Phys. Rev. B **38**, 9178 (1988).
- ²⁰J. Schneider, A. Handstein, I. Henke, K. Zavata, and T. Mydlarz, J. Phys. (Paris) Colloq. **41**, C8-682 (1980).
- ²¹P. Haasen, J. Non-Cryst. Solids **56**, 191 (1983).
- ²²S. Steeb and P. Lamparter, J. Phys. (Paris) Colloq. **46**, C8-247 (1985).
- ²³G. G. Whittle, A. M. Steward, and A. B. Kaiser, Phys. Status Solidi A **97**, 199 (1986).
- ²⁴S. Ikeda and Y. Ishikawa, J. Phys. Soc. Jpn. **49**, 950 (1980).
- ²⁵P. F. Sullivan and G. Seidel, Phys. Rev. **173**, 679 (1968).
- ²⁶G. Pepperl, D. Kraus, and K. Stierstadt, Phys. Lett. **31A**, 75 (1970).
- ²⁷M. E. Fisher and J. S. Langer, Phys. Rev. Lett. **20**, 665 (1968).
- ²⁸T. G. Richard and D. J. W. Geldard, Phys. Rev. Lett. **30**, 290 (1973); Phys. Rev. B **12**, 5175 (1975).
- ²⁹M. Ausloos, in *Magnetic Phase Transitions*, edited by M. Ausloos and R. J. Elliot (Springer-Verlag, Berlin, 1983).
- ³⁰A. Arrott and J. E. Noakes, Phys. Rev. Lett. **19**, 786 (1967).
- ³¹K. Westerholt, J. Magn. Magn. Mater. **66**, 253 (1987).
- ³²K. Westerholt and G. Sobotta, J. Phys. F **13**, 2371 (1983).
- ³³K. Westerholt, H. Bach, and R. Römer, J. Magn. Magn. Mater. **45**, 252 (1984).
- ³⁴K. Westerholt, Physica **130B**, 533 (1985).
- ³⁵K. Siratori, K. Kohn, H. Suwa, E. Kita, S. Tamura, and A. Tasaki, J. Phys. Soc. Jpn. **51**, 2746 (1982).
- ³⁶T. Hasiwa, E. Kita, K. Siratori, K. Kohn, and A. Tasaki, J. Phys. Soc. Jpn. **57**, 3381 (1988).
- ³⁷J. Wosnitza and H. V. Löhneysen, J. Phys. (Paris) Colloq. **49**, C8-1203 (1988).